

ABSTRACT

Title of Thesis: A HIGH ENERGY AND POWER DUAL-ION BATTERY

Boyu Wang, Master of Science, 2019

Thesis Directed By: Professor Chunsheng Wang,
Department of Chemical and Biomolecular
Engineering

As the alternative of Lithium-ion Batteries, Dual-Ion Batteries (DIBs), utilizing the intercalation mechanisms of anions into graphite cathode and cations into anode materials, have been proposed as a novel energy storage system for the long cycle life, low cost and environmental impact. However, due to the high potential of anions intercalation into graphite, electrolytes with high oxidizing stability are required. Herein, all-fluorinated electrolyte (1 M LiPF_6 in fluoroethylene carbonate (FEC)/ bis(2,2,2-trifluoroethyl) carbonate (FDEC)/ hydrofluoroether (HFE) 2:6:2 by volume) enables the DIB to be operated within a wide voltage window with excellent cycling stability. Moreover, $\text{Li}_2\text{TiSiO}_5$ anode material with high reversibility and proper working potential (0.28 V vs. Li^+/Li), which supports high-rate operation due to free of lithium dendrite compared with graphitic anode, is applied here. This dual ion cell (graphite // $\text{Li}_2\text{TiSiO}_5$) exhibits high cycling stability with 71% capacity retention after 500 cycles and excellent rate performance (15 C).

A HIGH ENERGY AND POWER DUAL-ION BATTERY

by

Boyu Wang

Thesis submitted to the Faculty of the Graduate School of the
University of Maryland, College Park, in partial fulfillment
of the requirements for the degree of
Master of Science
2019

Advisory Committee:
Professor Chunsheng Wang, Chair
Professor Nam Sun Wang
Professor Chen Zhang

© Copyright by
Boyu Wang
2019

Acknowledgements

I would like to acknowledge the support of my advisor, Prof. Chunsheng Wang. His hard work and critical thinking as a scientist encourage me to pursue my academic career with determination.

I would also thank Dr. Long Chen, Dr. Fudong Han, Dr. Ji Chen, Dr Pengfei Wang and all other lab partners in our group, for their guidance on my research study and support for my daily life.

At last, I would appreciate the love and care of my family, motivating me to live earnestly.

Table of Contents

Acknowledgements.....	ii
Table of Contents.....	iii
List of Tables.....	iv
List of Figures.....	v
Chapter 1: Introduction.....	1
1.1 The demand for novel energy storage system.....	1
1.2 The overview of lithium ion batteries.....	3
1.2.1 Introduction to lithium ion batteries.....	3
1.2.2 The working principle of lithium ion batteries.....	6
1.3 The overview of dual ion batteries.....	8
1.3.1 Introduction to dual ion batteries.....	8
1.3.2 Reaction mechanisms for dual ion batteries.....	11
1.3.3 Basic Construction of DIBs.....	13
Chapter 2: Materials preparation and analytical methods.....	20
2.1 Electrode fabrication.....	20
2.2 Electrolyte preparation.....	20
2.3 Cell assembling.....	20
2.4 Materials characterization.....	21
2.5 Electrochemical techniques.....	21
Chapter 3: Results and Discussion.....	22
3.1 SEM and XRD Characterization.....	22
3.2 Electrochemical tests of graphite cathode, Li ₂ TiSiO ₅ anode and full cell.....	24
3.2.1 Electrochemical performance of graphite cathode.....	24
3.2.2 Electrochemical performance of Li ₂ TiSiO ₅ anode.....	27
3.2.3 Electrochemical performance of Li ₂ TiSiO ₅ /graphite full cell.....	29
Chapter 4: Conclusion and future work.....	32
Bibliography.....	34

List of Tables

Table 3.1 Structure parameters of $\text{Li}_2\text{TiSiO}_5$	23
---	----

List of Figures

Fig 1.1 Ragone plot for different electrochemical systems	2
Fig 1.2 average discharge potentials and specific capacity of (a) intercalation-type cathodes, (b) conversion-type cathodes, (c) conversion type anodes, and (d) an overview for all types of electrodes.....	5
Fig 1.3 The working principle of lithium ion batteries.....	6
Fig 1.4 The working principle of dual ion batteries.....	11
Fig 1.5 Schematic illustration of different stages of intercalated graphite	14
Fig 3.1 XRD pattern of $\text{Li}_2\text{TiSiO}_5$ powder	23
Fig 3.2 SEM images of (a) natural graphite (3243) under low magnification; (b) natural graphite (3243) under high magnification; (c) $\text{Li}_2\text{TiSiO}_5$ under low magnification; (d) $\text{Li}_2\text{TiSiO}_5$ under high magnification	24
Fig 3.3 The charge/discharge profiles of graphite cathode.....	25
Fig 3.4 The cycling performance of graphite cathode	25
Fig 3.5 The rate performance of graphite cathode	26
Fig 3.6 The charge/discharge profiles of $\text{Li}_2\text{TiSiO}_5$ anode.....	27
Fig 3.7 The cycling performance of $\text{Li}_2\text{TiSiO}_5$ anode	28
Fig 3.8 The rate performance of $\text{Li}_2\text{TiSiO}_5$ anode.....	29
Fig 3.9 The charge/discharge profiles of $\text{Li}_2\text{TiSiO}_5$ /graphite dual ion batteries.....	30
Fig 3.10 The cycling performance of $\text{Li}_2\text{TiSiO}_5$ /graphite dual ion batteries.....	31
Fig 3.11 The rate performance of $\text{Li}_2\text{TiSiO}_5$ /graphite dual ion batteries.....	31

Chapter 1: Introduction

1.1 The demand for novel energy storage system

Energy is closely related to human civilization and social development. Since the 21st century, issues such as energy crisis and environmental pollution have increasingly become the obstruction of sustainable development in all countries of the world. The promotion and utilization of clean energy instead of fossil energy is imminent. However, natural resources such as solar, wind and tidal power generation is characterized by discontinuity of natural factors, from which the energy generated cannot be integrated into the current power grid on a large scale. Therefore, the development of large-scale energy storage equipment is a crucial part of the advance in clean energy.

On the other hand, the low capacity and charging speed of current commercialized batteries hinder the development of mobile electronic devices and electric vehicles. Serious safety accidents such as spontaneous combustion and explosion occur frequently during the charging or driving process of electric vehicles. High-performance, safe and environmentally-friendly mobile energy storage technology has become a challenge for the development of mobile digital devices and renewable energy vehicles.

Therefore, continual efforts have been made to exploit efficient, stable, safe and eco-friendly energy storage systems, for which lithium-ion batteries have emerged in order to satisfy the demand. High energy performance of such electrochemical systems can be observed on the Ragone curve representing the energy and power characteristics

of energy storage systems [1]. On the other hand, the energy storage devices need to provide high power density for systems such as electric vehicles. For this reason, supercapacitors with high power density and long working life have been greatly developed [2-4].

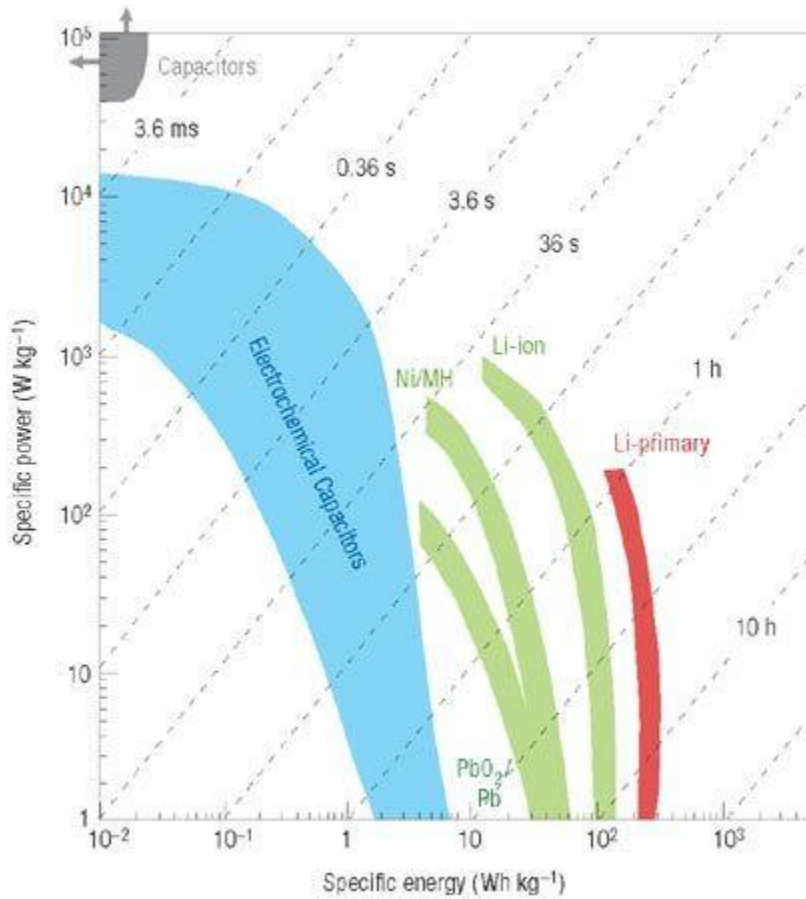


Fig 1.1 Ragone plot for different electrochemical systems [4]

However, several intrinsic problems have been found in either lithium ion batteries based on the intercalation and deintercalation chemistry of electrode materials, or supercapacitors based on the electric double layer theory or faradaic pseudocapacitance.

Despite of the relatively high energy density of former system, its power density is low due to the limitation of the Li ions transport in the solid hosts [5], while the supercapacitor system achieves high power density because of fast interface kinetics, of which the charge storage capacity is limited, resulting in its low energy density [6].

At present, realizing the energy storage system with both high energy density and high power density has been one of the crucial and difficult points in the field of materials science and electrochemistry [7].

1.2 The overview of lithium ion batteries

1.2.1 Introduction to lithium ion batteries

Lithium-ion batteries convert chemical energy into electrical energy for the energy supply of electrical devices, or store electrical energy obtain from natural resources in the form of chemical energy. In the industry, a typical battery pack is composed of multiple cell units (such as 18650 cylindrical cells, prismatic cells or pouch cells, etc.) in parallel, series or hybrid configurations to achieve the requirements of electrochemical performance such as voltage, capacity, power or energy, etc. Each cell consists of the positive electrode, negative electrode, separator, electrolyte and other accessories to ensure consistent electrochemical performance. The electrolyte in which a certain concentration of lithium salt is dissolved enables the transfer of lithium ions between the positive and negative electrodes, and the separator physically isolates the positive and negative electrodes to avoid internal short circuit.

In order to address the energy density issue arose in lithium-ion battery systems, the main idea is to develop novel positive and negative electrode materials with high specific capacity, high voltage and long cycle stability.

The types of materials that have been systematically studied for lithium-ion battery cathode are as follows: (1) intercalation materials, (2) conversion-type materials, and for lithium-ion battery anode are as follows: (1) graphite and hard carbons, (2) lithium titanium oxide, (3) alloying materials

Electrochemical properties of a cell (such as voltage window, charge and discharge capacity, coulombic efficiency, energy density, power density, etc.) are always related to the nature of the battery composition (cathode and anode active materials, electrolytes, separators). In general, the stability of the interface between the electrode materials and the electrolyte determines the cycle life and the safety of the battery. Compared to commercialized lead acid batteries or Ni-Cd batteries, rechargeable lithium battery technologies are constantly getting improved. Advances in technologies are mainly derived from both the internal chemistry and energy properties of the battery.

The development of novel intercalation materials relies on the innovation in solid-state electrochemical reactions, of which the ultimate goal is to meet the requirement of energy supply for modern portable devices. Fig 1.2 depicts the average electrode potential against experimental capacity (for anodes materials and intercalation cathodes materials) and theoretical capacity (for conversion cathodes materials). [8]

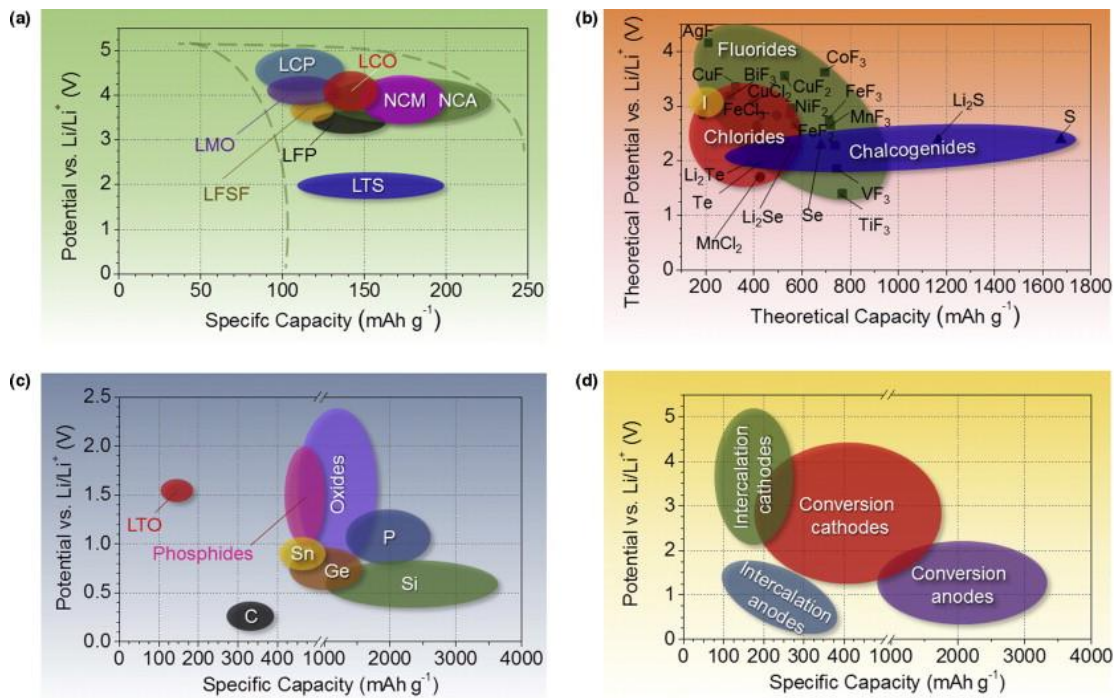


Fig 1.2 average discharge potentials and specific capacity of (a) intercalation-type cathodes, (b) conversion-type cathodes, (c) conversion type anodes, and (d) an overview for all types of electrodes. [8]

Whittingham first introduced a lithium metal secondary battery with lithium metal as the negative electrode and titanium disulfide as the positive electrode.[9] He demonstrated that the layered structure titanium disulfide enabled reversible charge and discharge of an electrochemical cell through intercalation chemistry. The commercialization of TiS₂ batteries was not successful due to a series of safety issues with lithium metal anode, which could form lithium dendrite, and the growth of lithium dendrite with cycles will fail the cell by internal short circuit and even cause latent fire hazard. Although scientists tried to avoid lithium dendrites by replacing lithium metal by lithium-aluminum alloy, the severe volume expansion of alloy electrodes during charge and discharge remained a problem. [10]

Goodenough and his co-workers studied the intercalation/deintercalation of lithium in lithium cobalt oxide and lithium nickelate with stable structure and proposed LiMO_2 (M is Co, Ni, Mn, etc.) compounds as electrode materials. Yazami and Touzain first reported the electrochemical lithiation and delithiation of graphite in 1982. These works resulted in the emergence of first-generation lithium ion battery (LiCoO_2 as the cathode and carbonaceous materials as the anode) by Akira Yoshino. [11]

1.2.2 The working principle of lithium ion batteries

Fig 1.3 shows the schematic diagram of a typical lithium ion cell, which consists of the graphite anode, the lithium cobalt oxide (LiCoO_2) cathode and the organic electrolyte. [12]

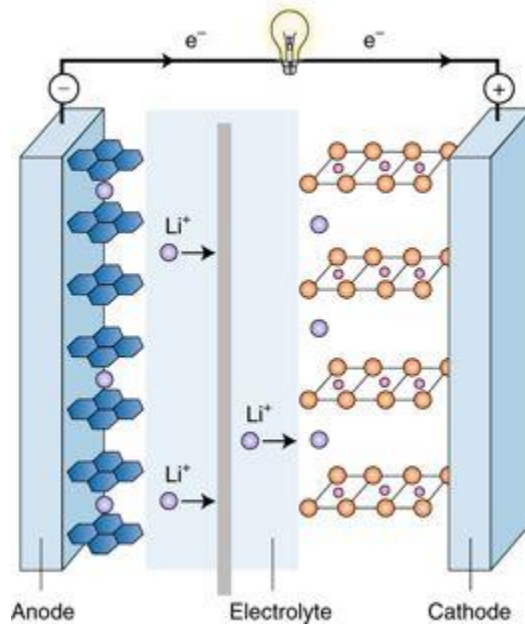
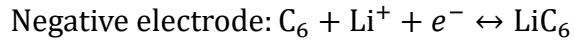
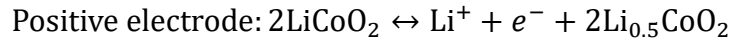


Fig 1.3 The working principle of lithium ion batteries [12]

Since the source of lithium ion in commercialized lithium ion batteries is the lithiated transition metal oxide and the salt of lithium in electrolyte, charging the cell

is the very first process of operation. During charging of the cell, lithium ions are released from lithiated cathode material, and insert into graphite anode, and the process is opposite during discharging. Since the lithium ions shuttle between cathode and anode as the charge carrier, and anions are not involved in the reactions, the total amount of ion keeps constant. Therefore, the lithium ion battery is also called rocking-chair battery. The half-cell reactions are: [13].



Within the first few cycles, the irreversible reaction on the electrode and electrolyte interface may form the passivation layer which prevent further irreversible reactions and protect the electrode materials to be stable.

In addition to the development of new energy storage materials, the progress in high-efficiency and low-cost energy storage devices is also one of the hot spots. A new type of energy storage system with graphite as both positive and negative electrode materials is developed, also known as dual graphite battery, with the feature of high working voltage, low cost and long cycle life. On this basis, a series of energy storage systems called dual ion batteries are developed, of which the positive and negative electrode materials are not limited to graphite, exhibiting better electrochemical performance than conventional lithium ion batteries. [14]

1.3 The overview of dual ion batteries

1.3.1 Introduction to dual ion batteries

At present, lithium ion secondary batteries occupy the main superiority in the energy storage market of portable electronic devices and electric vehicles. [15-21] Nevertheless, the current state-of-the-art lithium ion batteries provide narrow specific energy of around 200 Wh/kg with low specific power of 50 W/kg, [22–27] which is far from the minimum requirement of 350 Wh/kg specific energy with power to energy ratio (P:E) = 3 for electric vehicles. [28] Immense amount of work remains from the aspect of improving the energy and power density, capacity and cycle performance to satisfy the requirements of applications mentioned above.

Dual ion battery is the promising energy storage technology which is possible to meet the requirements of above applications. Also, replacing the lithiated transition metal oxide with graphite for cathode materials would be ideal for reducing the overall cost. [29]

In 1938, Rüdorff and Hofmann first reported anion intercalation of HSO_4^- from concentrated acid electrolyte into graphite as the cathode material for battery applications. [30] In 1989, Mc Cullough et al. first reported an energy storage system using dual graphite electrodes with a non-aqueous electrolyte. [31-34] In 1994, Carlin et al. studied the dual intercalation of cations and anions of ionic liquid electrolytes instead of lithium-based salt electrolytes. [35]

Since the size of the intercalated anion and cation is larger than the interlayer spacing of the graphite, the electrode structure is easily destroyed, resulting in poor

reversibility of the insertion/deinsertion electrochemistry and corresponding short battery life.

Thereafter, researchers started to pay attention to the reaction mechanism of anions [36-37] and cations [38-40] insertion/deinsertion electrochemistry, in particular the intercalation mechanism of lithium salt anion into graphite cathode. In 2000, Seel and Dahn investigated the insertion mechanism of hexafluorophosphate (PF_6^-) into graphite [41] Multiple stages of phase change was observed during the intercalation of PF_6^- ion into graphite.

In 2012, the concept of dual graphite battery was extended to dual ion battery by Placke et al. employing the lithium titanate anode with ionic liquid electrolyte. [42] As the conventional organic electrolyte would decompose at high potential due to highly oxidizing condition, which leads to insufficient coulombic efficiency and poor cycle life, replacing organic electrolyte with ionic liquid electrolyte is an alternative to the present systems.

In 2014, Read et al. first accomplished the simultaneous intercalation of lithium ion and PF_6^- anion into graphite anode and cathode. The cut-off voltage is up to 5.2 V contributed to the fluorinated electrolyte with additive can tolerate the high cut-off voltage up to 5.2 V, leading to a coulombic efficiency up to 97% at a rate of C/14. [43] In 2015, Lin et al. developed an ultrafast rechargeable system, introducing the concept of an aluminum metal anode for dual ion batteries. The battery is enabled by the redox reaction of aluminum at anode side and the insertion/deinsertion of chloroaluminate anions (AlCl_4^-) into graphite cathode.

Further efforts on inexpensive ion battery systems (such as Na^+ , K^+ , Ca^{2+} , Al^{3+} , etc.) have been made to reduce the cost of dual ion batteries. [32, 38, 44-45]

Different kinds of carbon materials have been studied for improving the positive electrode capacity and cycling stability, such as natural graphite, mesocarbon microbead (MCMB), highly oriented pyrolytic graphite (HOPG), etc.

Münster University battery research center (MEET) studied electrochemical insertion behavior of different anions (ClO_4^- , BF_4^- , PF_6^- , TFSI^- , FTFSI^- , FSI^- , AlCl_4^-), the specific capacity of different kinds of anion intercalated graphite materials is around 90 mAh/g. [46-52] However, due to the mismatch between the anion sizes and the graphite interlayer spacing, several cycles of charge and discharge test will cause volume expansion of the electrode, which results in the poor cycle performance. Specifically, because of the larger radius of intercalated anions in the cathode (4.36 Å for hexafluorophosphate), the related volume expansion causes structural damage of the graphite (3.36 Å for graphite) electrode.

It has been reported that a metal–organic framework with large specific surface area, three-dimensional pores, and adjustable structure can be used as the intercalation material. Since the tunnel-type metal–organic framework is adjustable, the porous structure can be modified to match the size of intercalation anions. A metal-organic framework, $\text{Fe}_2(\text{dobpdc})$, is synthesized for the cathode of the dual ion cell to undergo the reversible intercalation of weakly coordinating anions such as PF_6^- , presenting a stable cycling performance of 50 cycles with minor decay. [53]

The above studies show that the energy density of the dual ion battery is consistent with that of the lithium ion battery. However, the difficulty in slow reaction kinetics

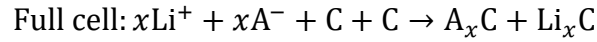
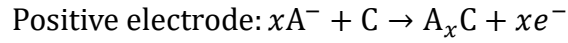
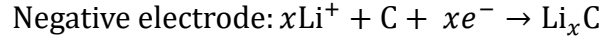
and low power density still exists due to the intercalation chemistry of lithium ion in graphite anode. Moreover, dendritic problems caused by overcharge of the battery or safety issues caused by high temperature or short circuit become the defects of such dual ion batteries.

Apart from the study of mechanism for dual ion batteries, few attempts have been made to develop new cathode and anode materials for dual ion batteries. Screening and matching proper electrode materials with moderate voltage plateaus and high stability is crucial in further advancing the position of the dual ion battery on the Ragone plot diagonally. Besides, the lack of deep understanding of the interaction between the inserted ions and insertion materials, the transport and kinetics of inserted ions in the insertion materials retards the development of dual ion batteries towards high energy density and high power density compatibility. In addition, the factors causing the stability degradation of dual-ion batteries needs to be further investigated. Research on the structural changes and the defects of the electrode materials after ion intercalation, along with the side reactions is required to improve the cycle life of the system.

1.3.2 Reaction mechanisms for dual ion batteries

Different from the conventional rocking-chair lithium ion batteries in which only lithium ions shuttle between two electrodes, in dual ion batteries, both the cations and anions are involved in the reaction. During the charge process, the cations intercalate into the negative electrode, and the anions intercalate into the positive electrode; while in the discharge process, both the cations and anions in the electrodes are released back into the electrolyte. The charge and discharge mechanism of a dual ion cell using graphite as both cathode and anode material is shown in Fig 1.4. For a case of a dual

ion battery with graphite as the positive and negative electrodes, and lithium salt solution as the electrolyte, the cell reactions are as follows:



where C stands for graphite cathode and anode, A^- stands for anions in the electrolyte.

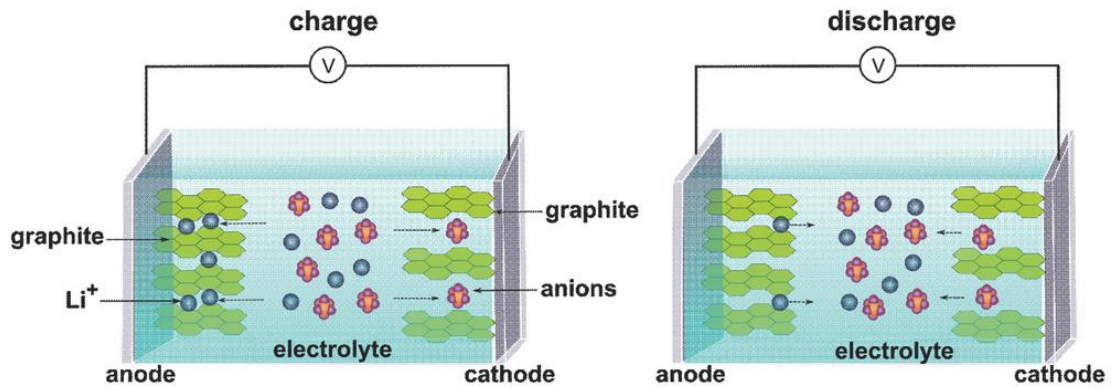


Fig 1.4 The working principle of dual ion batteries [54]

Since both the cations and anions react at the electrodes, the concentration of ions is reduced during charge and recovered during discharge. The potential differences between lithium ion battery and dual ion battery has been studied by Seel and Dahn. [41] The cell potential of dual ion battery can be expressed as

$$-neV = n(\mu_{\text{Li}} - \mu_{\text{Li}^+}) + n(\mu_{\text{A}} - \mu_{\text{A}^-})$$

where n is the quantity of lithium and anion species involved in the cell reaction; μ_{Li} represents the chemical potential of lithium component in the anode material and μ_{Li^+} represents the concentration dependent chemical potential of lithium ion in the electrolyte. The definition of μ_{Li} and μ_{Li^+} are the corresponding quantities for the anion

component in the cathode material and electrolyte. According to the Nernst equation, the equilibrium potential of the cell is concluded as

$$-neV = \mu_{Li} + \mu_A - \mu_{Li^+}^0 - \mu_{A^-}^0 - 2kT \ln(Li^+)$$

where $\mu_{Li^+}^0$ and $\mu_{A^-}^0$ are the standard chemical potentials of ions in the electrolyte.

From the equation above, some inferences can be found. Since the cations and anions in the solution participate in the full cell reaction, the potential of dual ion batteries may depend on the solvent and the type of anion. Furthermore, the concentration term of ionic species in the Nernst equation reveals that the potential of dual ion batteries varies with the electrolyte concentration.

1.3.3 Basic Construction of DIBs

1.3.3.1 Cathode materials

Inorganic materials

Graphite generally consists of polyaromatic rings formed by carbon atoms of sp^2 hybridization. The overlap of $2p_z$ orbitals of carbon atoms forms the π -electronic network. The planar layer composed by aromatic rings is named the basal plane. The spacing of carbon atoms in the layer is 0.142 nm. The interaction between layers of graphite by van der Waals force results in the ABAB stacking order (hexagonal graphite) or the ABCABC stacking order (rhombohedral graphite) of graphene layers. Different synthesis methods can control and adjust the interlayer spacing of graphite. [55-56] The bonding strength between graphene layers is weak (the bond energy of van der Waals force is 16.7 kJ/mol), which provides space for the insertion of ions or ion clusters. The intercalated ions occupy the space between graphite layers in the vertical

direction to form intercalated layers. The insertion status of ions into graphite is termed “stage”, which refers to the number of graphite layers between alternate layers of intercalated ions. Fig 1.5 shows the stage 1, stage 2 and stage 4 schematically. [54] The graphite intercalation compounds tend to form low order stages with relatively high potential, leading to the increase in intercalated anions and higher capacity.

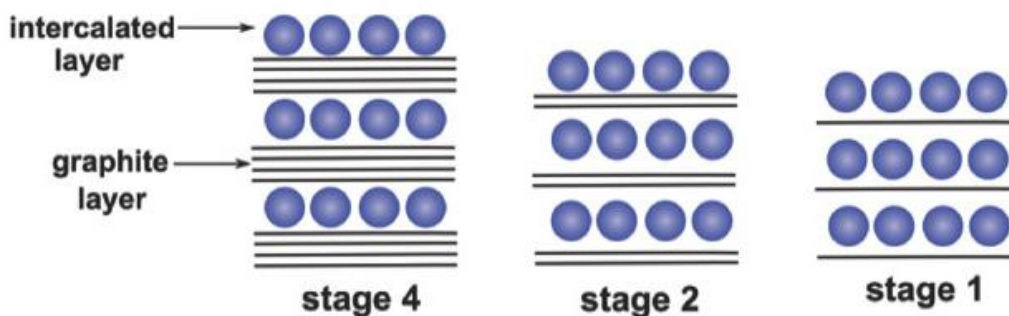


Fig 1.5 Schematic illustration of different stages of intercalated graphite [54]

Santhanam and Noel investigated the intercalation/deintercalation of ClO_4^- into graphite. A graphite composite containing 20 wt.% of polypropylene as the binder is proved to be more efficient than commercialized graphite materials. [37]

Ishihara et al. studied the intercalation/deintercalation of PF_6^- into different kinds of carbon cathode materials, which presents the specific charge and discharge capacity of carbon materials intercalated by PF_6^- within the voltage window of 3.5-4.9 V. [57] The charge and discharge capacities vary with different kinds of graphite intercalation compounds formed through insertion of PF_6^- into multiple carbon sources. For carbon materials with high surface area, the electrochemical reversibility is poor; while graphite materials with diameters of 4 and 6 μm , the reversible capacity is relatively

high, suggesting that the graphitization degree may be important for reversible intercalation.

Placke et al. studied the intercalation performance of bis(trifluoromethanesulfonyl) imide anions (TFSI⁻) in graphite at 20°C and 60 °C. [50] The test data shows that the graphite materials with relatively small particle diameter and high specific surface presents high discharge capacity, such as KS4 or KS6L; whereas the mesocarbon microbead (MCMB) with surface coating, by which the insertion of anions with large size (TFSI⁻) may be impeded, presents the lowest discharge capacity. Furthermore, the excellent discharge specific capacity performance (91~110 mAh/g) of various graphite materials at 60 °C indicates the better mobility and intercalation ability of TFSI⁻ at high temperatures.

Organic materials

Apart from graphite materials, other cathode materials such as organic materials are developed for dual ion battery systems as well, because of the wide range of eligible raw materials, moderate synthesizing temperature, less pollution and renewability of the waste and the low cost of the process. [58-65] Various organics have been used as active materials for batteries, such as conducting polymers, organic disulfides, radical polymers and carbonyl compounds. [63] Different from graphitic cathode materials for dual ion batteries, the mechanisms for organic cathode materials involve the doping, redox or bond forming/breaking process. [66-67]

Speer et al. studied the organic polymer thianthrene-functionalized polynorbornenes as the cathode material for dual ion cells. [68] The thianthrene material is oxidized to form radical cation during charge, and reacts with negative

charge carrier such as PF_6^- to realize the insertion of anions. This process goes through two steps. The potential plateaus for the first oxidation step of thianthrene is 4.09 V (vs Li/Li⁺). While the first step reveals the high potential plateaus and reversible reaction of thianthrene to serve as the high-voltage material, the second step was only detected under extremely dry conditions. [69-71] Although the material presented a capacity of up to 66 mAh/g, the capacity decayed fast 100 cycles, revealing poor cycling performance.

In addition to organic polymers, organic non-polymeric materials can be the candidate for intercalation cathode materials. Deunf et al. investigated the electrochemical intercalation chemistry of a layered structure aromatic amine, dilithium 2,5-(dianilino) terephthalate (Li₂DAnT). Electrolytes containing anions such PF_6^- , ClO_4^- , and TFSI⁻ were proved to be inserted in this cathode materials reversibly. The best cycling performance was observed with the electrolyte of 1 m LiClO₄ dissolved in PC. A kind of polycyclic aromatic hydrocarbon, coronene, was reported to support for PF_6^- intercalation in standard carbonate electrolyte, delivering a stable capacity of ~40 mA h/g. [61] This material was also reported to function in a sodium-based dual ion battery with a wide temperature window of -20 to 40 °C and excellent capacity retention. [72].

Although most of the organic materials developed for dual ion batteries are not comparable in capacity to graphite cathodes so far, the diverse mechanisms for the organic materials present the potential of for the capacity growth.

1.3.3.2 Anode materials

The capacity performance of graphite anode is confined by the few amount of crystallographic sites for the storage of charge carrier ions. Therefore, the demand for developing new materials with more insertion sites or new reaction chemistry to replace conventional intercalation materials has emerged. Electrochemical fundamentals and applications of dual ion cells based on solid state reactions, such as alloying and conversion reactions, or gas phase reactions have been studied for the potential for breaking the energy density limit of intercalation materials. [73-74]

Gunawardhana et al. developed a dual ion cell system with MoO₃ anode and graphite cathode. [75] The energy storage was accomplished through the Li⁺ insertion into MoO₃ anode and PF₆⁻ insertion into graphite cathode, respectively. The cell displayed a discharge capacity of 81 mAh/g for the first cycle and good cycling performance of 90% capacity retention after 200 cycles. The tests of different factors in operation were conducted to study their effect on the cell performance, such as voltage range, rate performance, operating temperature and the ratio between cathode and anode. [76]

Shi et al. reported a novel dual ion cell system consisting of reduced graphene oxide anode, graphite cathode and ionic liquid electrolyte of (EMIm)⁺(PF₆)⁻. [77] Instead of conventional intercalation chemistry, the anode reaction mechanism relies on the adsorption of EMIm⁺ cation on the surface of RGO electrode.

1.3.3.3 Electrolyte

The electrolyte is critical for dual ion cells, for the reason that ions in the electrolyte function not only as the charge carrier but also as the active material for the

charge storage in the electrodes. Because of the high working voltage of dual ion batteries, high requirements of electrolytes were proposed: a wide electrochemical window to simultaneously satisfy the low anodic potential and cathodic potential without decomposition, high ionic conductivity, a wide temperature range, etc. Existing dual ion electrolytes can be classified into organic liquid electrolytes and ionic liquid electrolytes.

Organic electrolyte is widely used in lithium ion batteries and attempts to employ it in dual ion batteries are also made. The common lithium salt in electrolytes are LiClO_4 、 LiAsF_6 、 LiBF_4 、 LiPF_6 and LiTFSI . Major solvents should process high dielectric constants and solubilities of lithium salt.

Seel and Dahn studied the intercalation manner of PF_6^- into graphite in organic electrolytes, ethyl methyl sulfone (EMS) and ethylene carbonate/diethyl carbonate mixture (EC/DEC), and determined the potential for staging transitions and the compositions for different stages. They believed that the graphite intercalation compound of stage 2' is $(\text{PF}_6)_{0.5}\text{C}_8$, delivering a theoretical capacity of 140 mAh/g, although the experiment data indicated that the compound is between $(\text{PF}_6)_{0.5}\text{C}_{14}$ and $(\text{PF}_6)_{0.5}\text{C}_8$. [41]

Fluorinated solvent of the electrolyte usually displays high oxidation stability. [78-79] Read et al. developed a fluorinated electrolyte system to operate the dual graphite cell at high cut-off voltage of 5.2 V. by employing fluorinated solvent fluoroethylene carbonate (FEC) with fluorinated additive. [43] The FEC-based electrolyte exhibited improved cycling stability for 200 cycles compared to

nonfluorinated electrolyte, resulting from the higher oxidation potential of the fluorinated component.

Ionic liquids, which are salts with room temperature melting points, provide high thermal stability, redox reaction stability and a wide electrochemical window. [80-82]

Rothermel et al. developed bisalt ionic liquid electrolyte Pyr14TFSI-LiTFSI with additive ethylene sulfite (ES) to intentionally form solid electrolyte interphase (SEI). [36] The formation of SEI film on the surface of graphite electrodes allows the insertion of lithium ion and TFSI⁻ anion, while preventing the insertion of Pyr14⁺ cations and other large molecules. The capacity of the cell containing electrolyte with ES additive rose to 97 mAh/g, about twice as much as the cell with no electrolyte additive. This approach enabled the highly reversible insertion/deinsertion of target ions, which enhanced the cycling stability with high coulombic efficiency while maintaining the energy density at around 85%.

Chapter 2: Materials preparation and analytical methods

2.1 Electrode fabrication

$\text{Li}_2\text{TiSiO}_5$ powder was used for anode active materials and graphite grade 3243 was used for cathode active materials. The cathode active material was thoroughly mixed with carbon black as the conductive additive and polyvinyl difluoride (dissolved in N-methyl-2-pyrrolidone, NMP) as the binder at a weight ratio of 8:1:1. The mixture was pasted onto an aluminum foil as the current collector. The anode electrode material was fabricated through the same procedure and pasted onto a copper foil as the current collector. The electrode foil was then dried in a vacuum oven at 100°C overnight. Then, the foil was pressed by an electrode calendaring machine. The pressed foil was punched by 1/2 inch in diameter, then weighed and collected as the testing electrodes.

2.2 Electrolyte preparation

The solvent of the electrolyte was a mixture of fluoroethylene carbonate/3,3,3-fluoroethylmethyl carbonate/1,1,2,2-tetrafluoroethyl-2',2',2'-trifluoroethyl ether (FEC: FEMC: HFE, 2:6:2 by volume). The all-fluorinated electrolyte was made by dissolving 1M lithium hexafluorophosphate (LiPF_6) in the mixed solvent.

2.3 Cell assembling

Coin cells for half-cell test were assembled by stacking the as-prepared positive or negative electrode, a separator (Celgard 3501) and lithium metal foil as the counter electrode with about 60 μL all-fluorinated electrolyte prepared above. Coin cells for

full-cell test were made up of $\text{Li}_2\text{TiSiO}_5$ anode and graphite cathode following the same procedure.

2.4 Materials characterization

To obtain the surface topography information of $\text{Li}_2\text{TiSiO}_5$ powder and natural graphite (3243), scanning electron microscope (SEM) characterization was performed for these two materials on a Hitachi SU-70 ultrahigh resolution fieldemission SEM.

X-ray diffraction (XRD) is the technique to conduct qualitative and quantitative analysis of the structure of powder samples based on the position and intensity of the peak. The X-ray diffraction (XRD) test for analyzing the crystal structure of $\text{Li}_2\text{TiSiO}_5$ powder the was performed on a Bruker D8 Advance system, using Cu-K α radiation in the 2θ range of 15° - 90° .

2.5 Electrochemical techniques

Constant current charge-discharge is the technique for testing the charge/discharge curve and cycle life of batteries. The charge and discharge process are conducted at a constant value of current density until the cut-off voltage is reached. The time variable t can be converted to the capacity Q through the following relationship:

$$Q = It$$

where I refer to the constant current.

Then the voltage-capacity curve and capacity as a function of cycle number are obtained. The electrochemical performance was tested by using an Arbin battery test station and a LAND battery test system.

Chapter 3: Results and Discussion

3.1 SEM and XRD Characterization

Currently, the common anode materials for dual ion batteries are dominated by graphite. However, the low potential plateaus of cation intercalation of graphite increase the risk of safety issues, due to the lithium dendrite formation at high current density. Though the spinel-structured material, lithium titanate, have exhibited high cycling stability and high coulombic efficiency as the DIB anode material, its low capacity and much higher potential compared with graphite anode limit the improvement in energy density.

Liu et al. studied the reaction mechanism of a new type of titanate material $\text{Li}_2\text{TiSiO}_5$. [83] They found a two electron ($\text{Ti}^{4+}/\text{Ti}^{2+}$) reaction was involved in the lithium storage process of $\text{Li}_2\text{TiSiO}_5$, forming TiO and Li_4SiO_4 at reduction state to store two lithium ions, which delivers a high theoretical capacity of 308 mAh/g and excellent cycling performance at a low working voltage (0.28 V vs. Li^+/Li).

In this research, $\text{Li}_2\text{TiSiO}_5$ powder was used for anode active material. XRD test was performed in order to verify the structure and crystallinity of the $\text{Li}_2\text{TiSiO}_5$ particles. (Fig 3.1) Evident crystalline peaks are shown in the XRD patterns, implying that the $\text{Li}_2\text{TiSiO}_5$ is highly crystallized, matching the characteristics of the crystalline $\text{Li}_2\text{TiSiO}_5$ reported by Liu et al.,[83] which indicated the tetragonal structure of $\text{Li}_2\text{TiSiO}_5$ with P4/nmm space group. The lattice parameters are shown in Table 3.1.

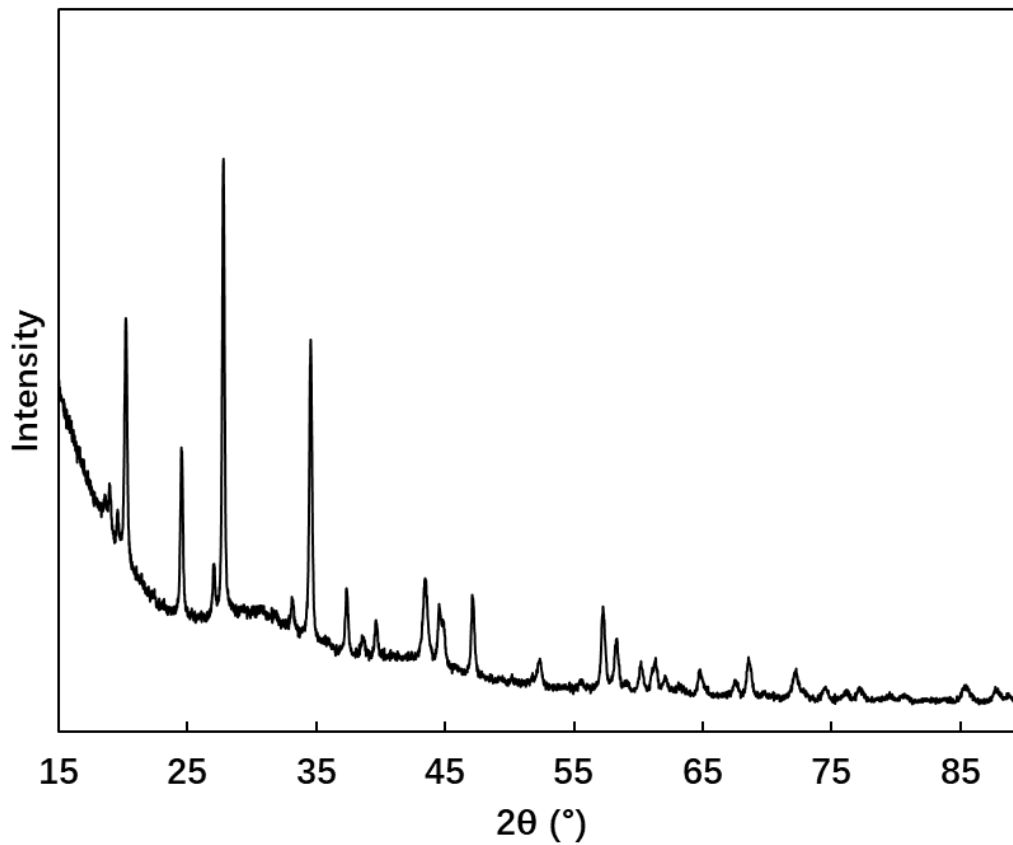


Fig 3.1 XRD pattern of $\text{Li}_2\text{TiSiO}_5$ powder

Table 3.1 Structure parameters of $\text{Li}_2\text{TiSiO}_5$

Compound	a	b	c	vol
$\text{Li}_2\text{TiSiO}_5$	6.4415 Å	6.4415 Å	4.4072 Å	182.87 Å ³

The morphologies of $\text{Li}_2\text{TiSiO}_5$ and natural graphite (3243) were observed through a scanning electron microscope (SEM), as shown in Fig 3.2. The raw $\text{Li}_2\text{TiSiO}_5$ particles displayed irregularly shapes within a size range of a few microns, whereas the graphite particles presented the clear flake structure measuring dozens of microns.

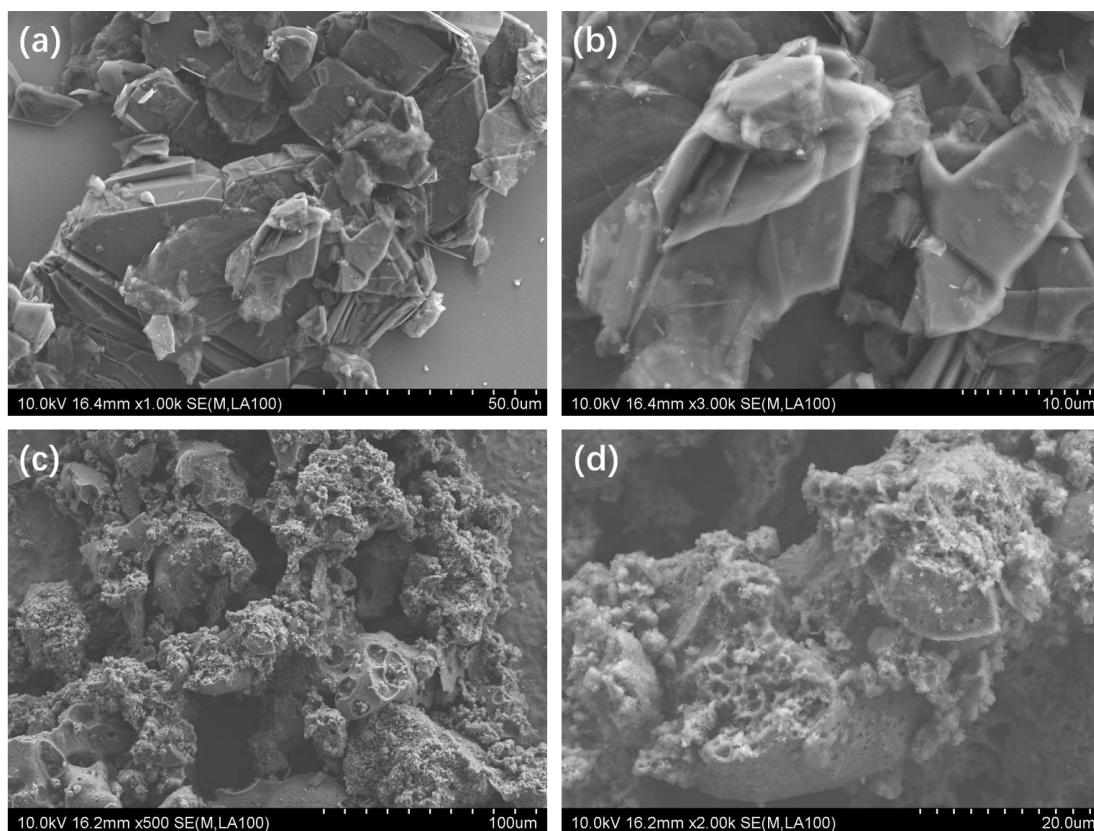


Fig 3.2 SEM images of (a) natural graphite (3243) under low magnification; (b) natural graphite (3243) under high magnification; (c) $\text{Li}_2\text{TiSiO}_5$ under low magnification; (d) $\text{Li}_2\text{TiSiO}_5$ under high magnification.

3.2 Electrochemical performance of graphite cathode, $\text{Li}_2\text{TiSiO}_5$ anode and full cell

3.2.1 Electrochemical performance of graphite cathode

The electrochemical performance of graphite cathode was evaluated by half-cell tests using lithium metal for counter electrode and all-fluorinated electrolyte. The specific capacity was calculated based on graphite active material.

The charge/discharge curve of graphite cathode at the current density of 1A/g is shown in Fig 3.3 and the excellent long-term cycling performance at the current density of 1A/g is shown in Fig 3.4.

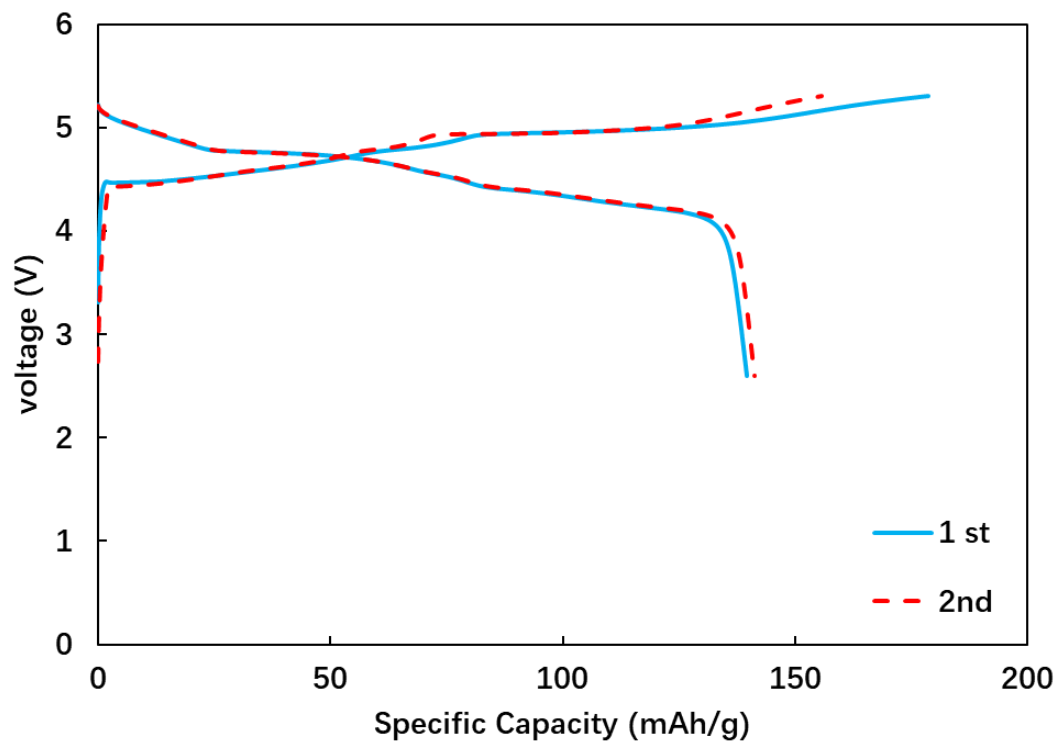


Fig 3.3 The charge/discharge profiles of graphite cathode

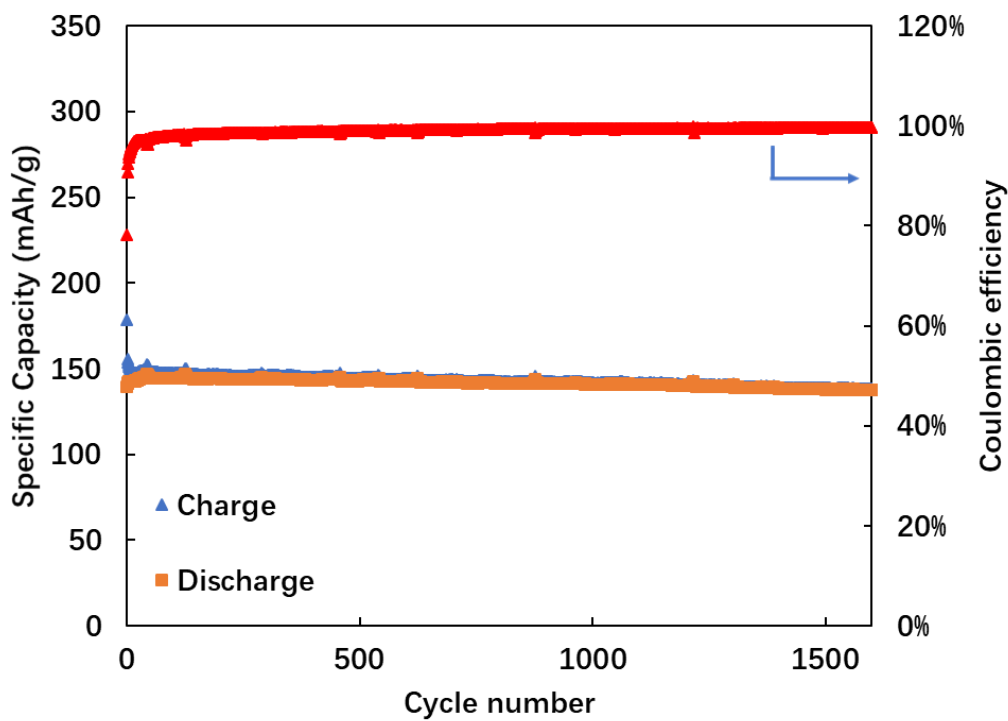


Fig 3.4 The cycling performance of graphite cathode

The graphite cathode exhibited an initial charge specific capacity of 178 mAh/g with two approximate potential plateaus at around 4.7 V and 5.0 V and then stabilized to around 140 mAh/g. For discharge process, potential plateaus at around 4.8 V and 4.4 V was observed, delivering an initial discharge specific capacity of 140 mAh/g. The reversible capacity retention was about 140 mAh/g after 1600 cycles with a coulombic efficiency of up to 99.6%. The limited decline in the capacity demonstrated the superior cycling stability of natural graphite (3243) as the anion intercalation material.

The graphite cathode displayed high rate capability as well. As shown in Fig 3.5, almost no capacity decline was observed ranging from the current density of 0.05 A/g to 0.5 A/g, and the specific capacity remained 118 mAh/g at a high current density of 5 A/g and was restored to the same level of beginning with the current density back to 0.05 A/g, which revealed the excellent kinetics of the intercalation chemistry of natural graphite (3243).

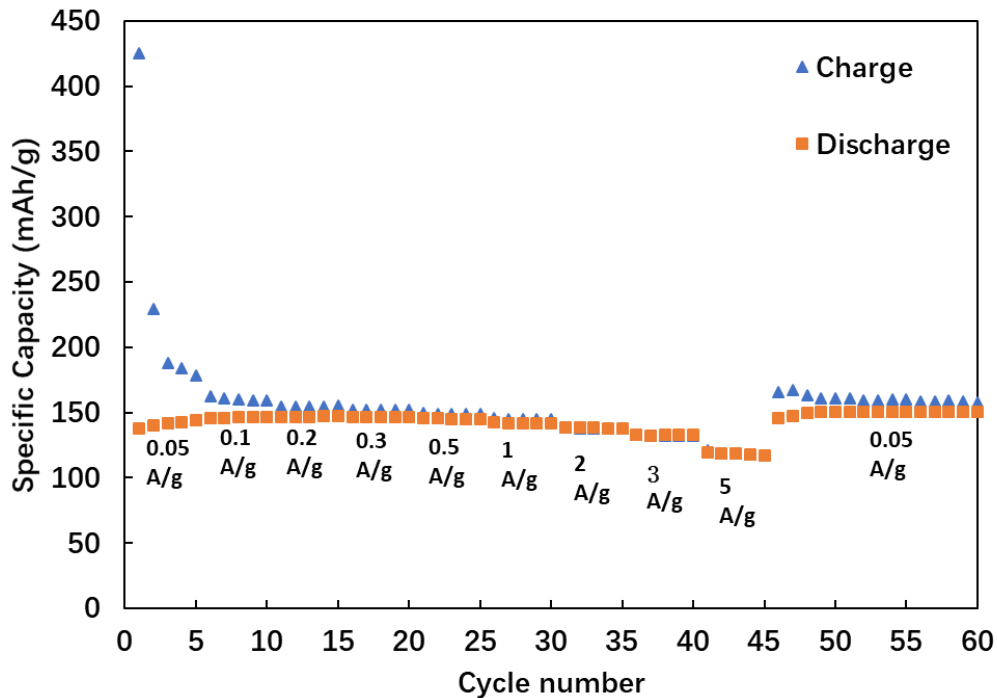


Fig 3.5 The rate performance of graphite cathode

3.2.2 Electrochemical performance of $\text{Li}_2\text{TiSiO}_5$ anode

The electrochemical measurement of $\text{Li}_2\text{TiSiO}_5$ anode materials followed the same procedure of graphite cathode. The specific capacity was calculated based on $\text{Li}_2\text{TiSiO}_5$ active material.

The charge/discharge curve of $\text{Li}_2\text{TiSiO}_5$ anode at the current density of 1A/g is shown in Fig 3.6 and the excellent long-term cycling performance at the current density of 1A/g is shown in Fig 3.7.

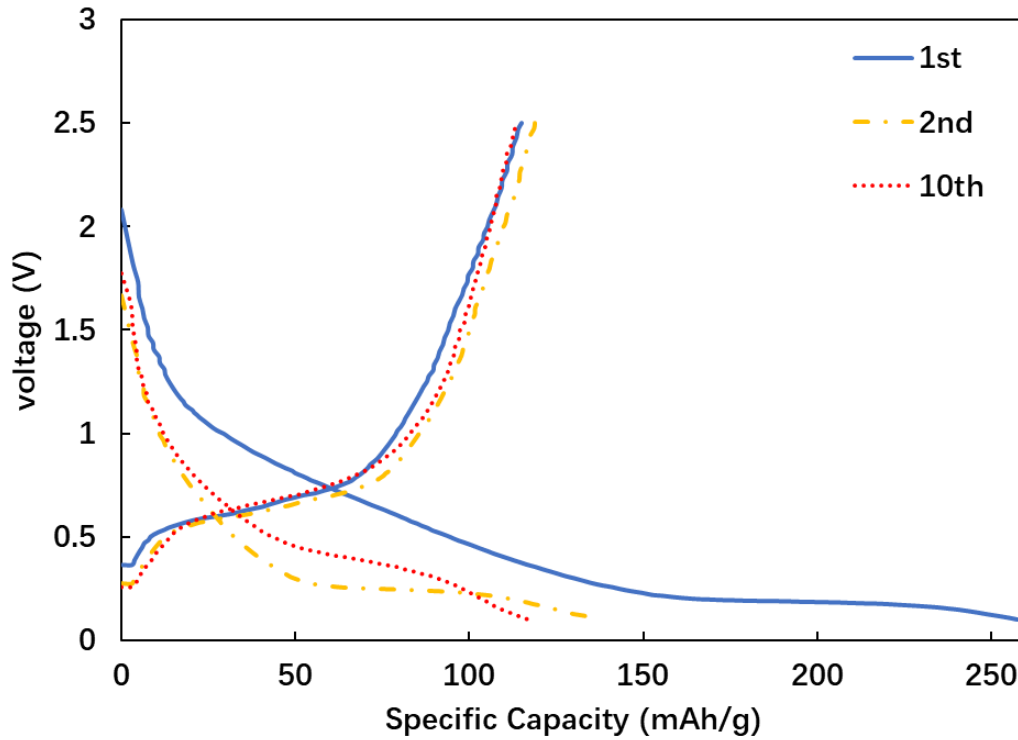


Fig 3.6 The charge/discharge profiles of $\text{Li}_2\text{TiSiO}_5$ anode

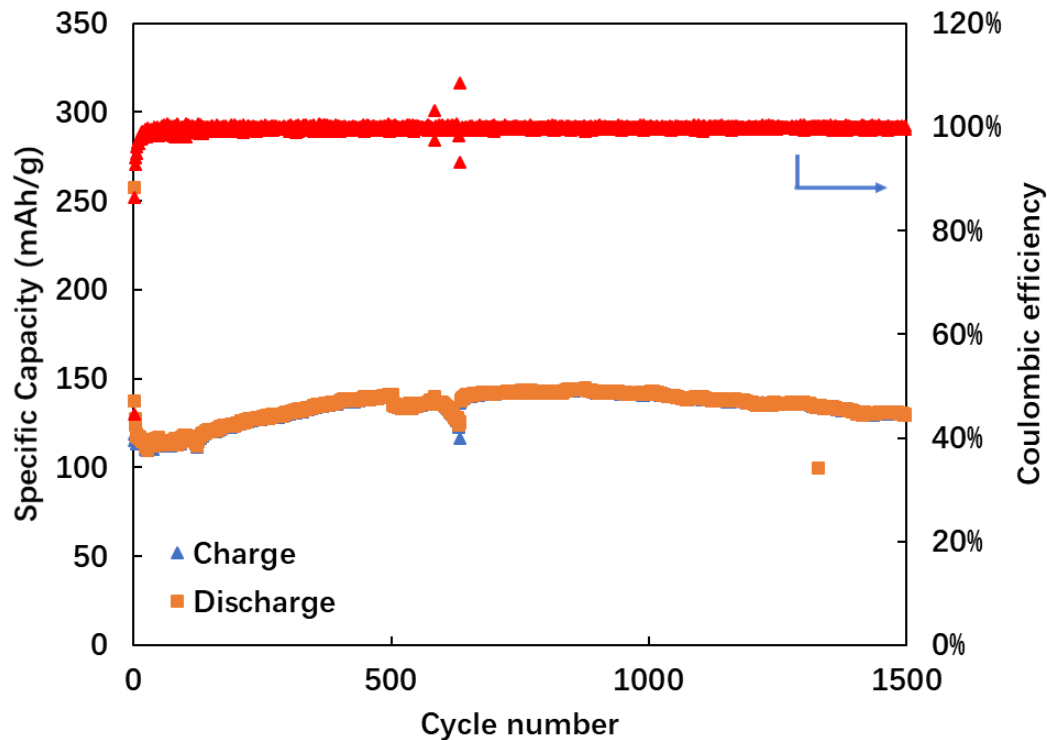


Fig 3.7 The cycling performance of $\text{Li}_2\text{TiSiO}_5$ anode

The potential plateaus of reduction and oxidation are located at 0.3 and 0.6 V, respectively. Moreover, the $\text{Li}_2\text{TiSiO}_5$ anode presented a large initial discharge capacity of 257 mAh/g, and which deliver a stable value of capacity with 150 mAh/g after 150 cycles. After 1500 cycles, the specific capacity remained 130 mAh/g. For the first use of $\text{Li}_2\text{TiSiO}_5$ anode in the dual ion battery system, the remarkable cycling performance is comparable to that in the lithium ion battery system.

The $\text{Li}_2\text{TiSiO}_5$ anode also displayed excellent rate performance. (Fig 3.8) The specific capacity of over 160 mAh/g was observed at a current density of 0.05 A/g, and half of the capacity was retained at the highest current density of 5 A/g, demonstrating that the $\text{Li}_2\text{TiSiO}_5$ anode was capable of constructing full cell with graphite cathode.

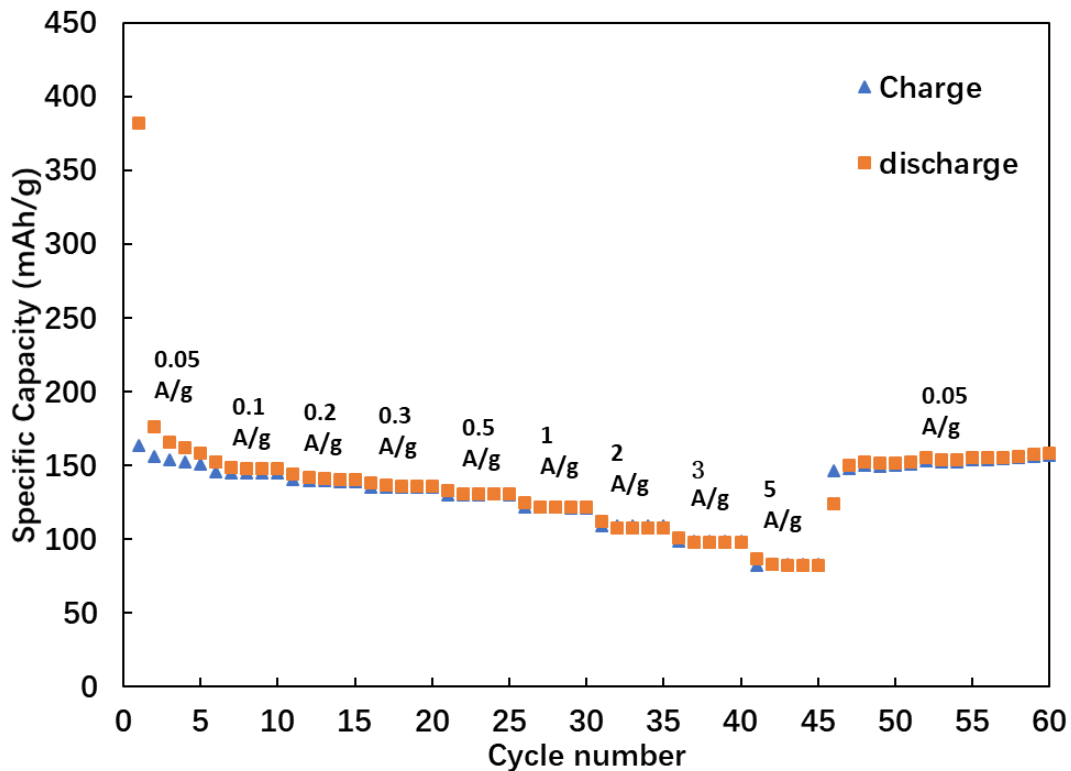


Fig 3.8 The rate performance of $\text{Li}_2\text{TiSiO}_5$ anode

3.2.3 Electrochemical performance of $\text{Li}_2\text{TiSiO}_5$ /graphite full cell

Since the low initial coulombic efficiency and large initial irreversible capacity of $\text{Li}_2\text{TiSiO}_5$ anode, a pre-cycle process to eliminate irreversible capacity was conducted for $\text{Li}_2\text{TiSiO}_5$ anode in order to reduce the capacity loss and achieve high cycling stability of full cell. The full cell tests were performed with capacity matching of anode and cathode, and the anode capacity surpassed 20% of the cathode capacity. The setting of cut-off voltages was also based on the capacity of anode and cathode.

Fig 3.9 shows the galvanostatic charge and discharge curves of the full cell. An irreversible specific capacity of around 90 mAh/g was observed during the first discharge process. Fig. 3.10 shows the rate performance of the full cell. With a range of current density from 0.05 A/g to 1 A/g, the full cell retained the good rate capability.

A supreme long-term cycling performance was also presented at a high current density of 1 A/g. The reversible capacity retained 71% for over 500 cycles with high coulombic efficiency up to 99.5%. (Fig. 3.11)

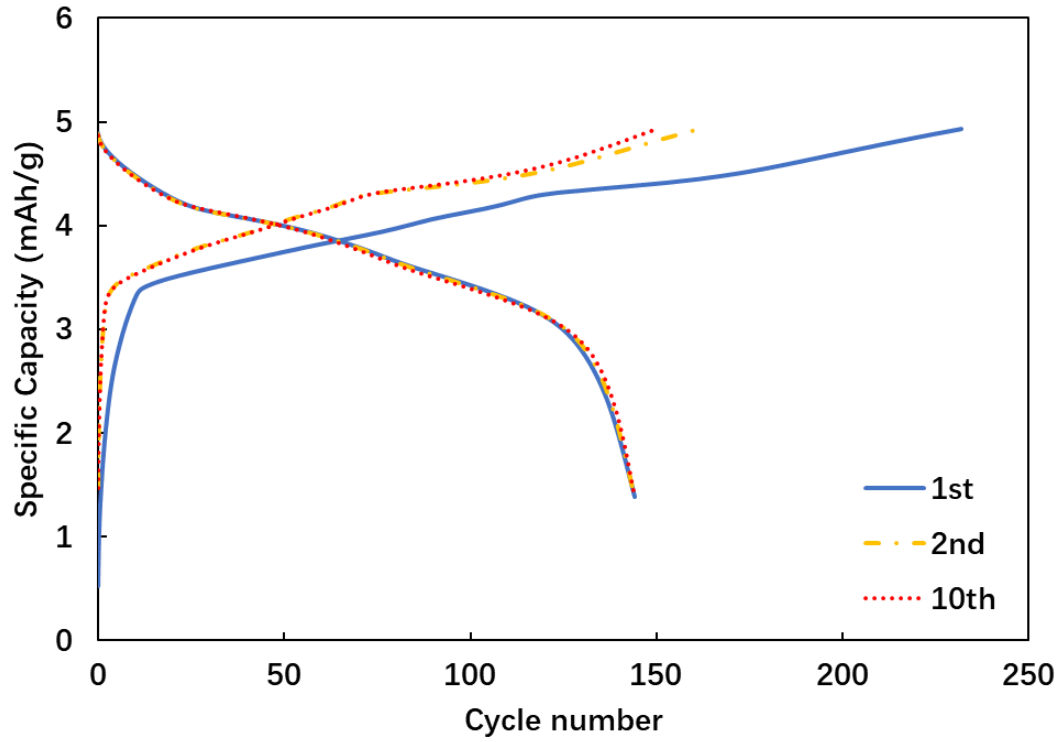


Fig 3.9 The charge/discharge profiles of $\text{Li}_2\text{TiSiO}_5$ /graphite dual ion batteries

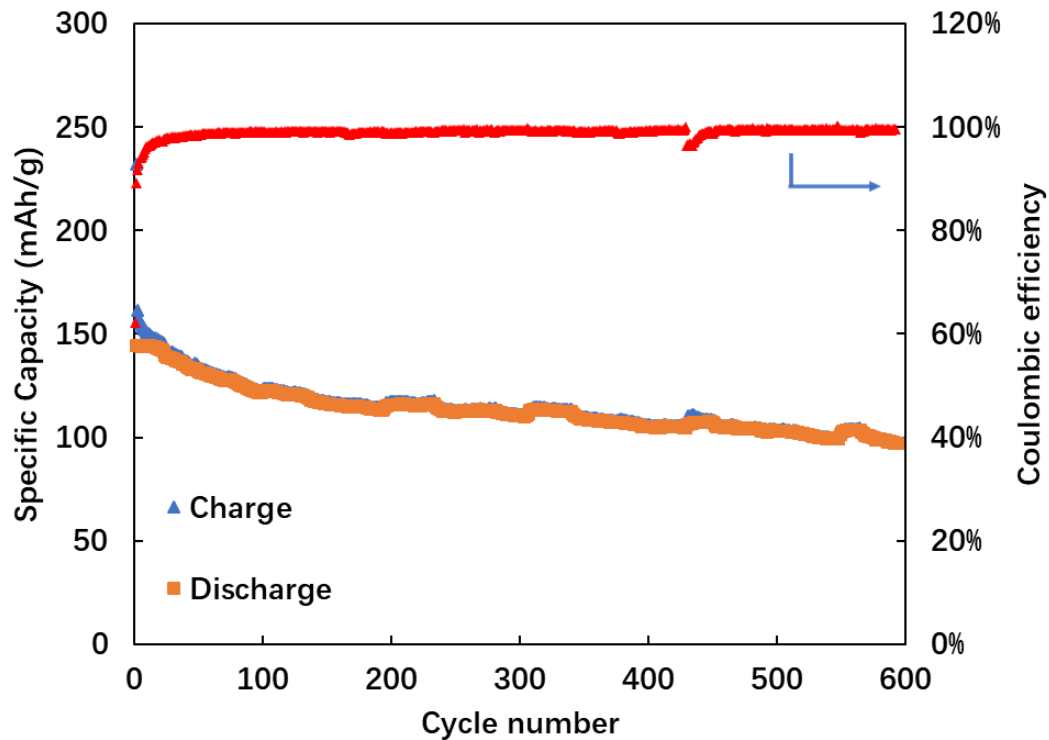


Fig 3.10 The cycling performance of $\text{Li}_2\text{TiSiO}_5/\text{graphite}$ dual ion batteries

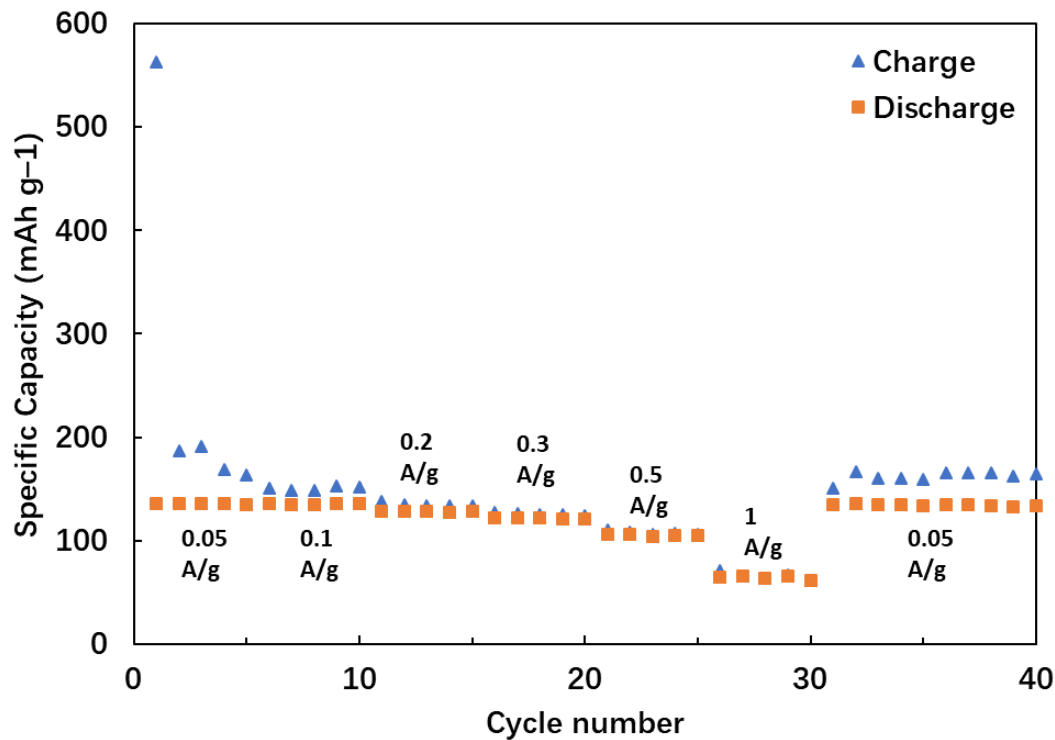


Fig 3.11 The rate performance of $\text{Li}_2\text{TiSiO}_5/\text{graphite}$ dual ion batteries

Chapter 4: Conclusion and future work

In this work a novel dual ion battery system was developed. The cathode chemistry is based on the reversible intercalation of PF_6^- anion into natural graphite (3243) cathode with a high cut-off voltage of 5.3 V, which is attributed to the enhanced oxidation stability of the all-fluorinated electrolyte (FEC:FEMC:HFE, 2:6:2 by volume). A new anode material $\text{Li}_2\text{TiSiO}_5$ was first introduced to the construction of a dual ion battery. $\text{Li}_2\text{TiSiO}_5$ anode exhibited a low discharge potential plateau of 0.28 V vs. Li^+/Li , providing a wide range of voltage window for the operation of full cell; meanwhile, the relatively higher potential plateau than lithium plating suppressed the formation of lithium dendrite and thus enabled a rise in rate capability without safety concern.

Both the cathode and anode materials presented excellent cycling stability. The reversible specific capacity of graphite cathode retained around 140 mAh/g after 1600 cycles and that of $\text{Li}_2\text{TiSiO}_5$ anode retained 130 mAh/g after 1500 cycles. Furthermore, $\text{Li}_2\text{TiSiO}_5$ anode achieved the specific capacity of over 160 mAh/g at the current density of 0.05 A/g and retained half of the specific capacity at the current density of 5 A/g. The specific capacity of graphite cathode kept stable at a range of current density from 0.05 A/g to 0.5 A/g and retained 118 mAh/g at 5 A/g. The remarkable rate and cycling performance of both anode and cathode using the all-fluorinated electrolyte enabled the stable operation of the full cell.

Further work is needed to eliminate the large irreversible capacity of the $\text{Li}_2\text{TiSiO}_5$ anode. One of the feasible methods is to introduce Li-rich materials with little reversibility like Li_2CuO_2 [84] into the graphite cathode as the supplement of lithium

ion source. Moreover, to reach high energy density for industrial application, concentrated and low-cost electrolytes should be developed for dual ion battery systems.

Bibliography

- [1] Bruce, P. G., Freunberger, S. A., Hardwick, L. J., & Tarascon, J. M. (2012). Li–O₂ and Li–S batteries with high energy storage. *Nature materials*, *11*(1), 19.
- [2] Choi, N. S., Chen, Z., Freunberger, S. A., Ji, X., Sun, Y. K., Amine, K., ... & Bruce, P. G. (2012). Challenges facing lithium batteries and electrical double-layer capacitors. *Angewandte Chemie International Edition*, *51*(40), 9994-10024.
- [3] Jiang, H., Lee, P. S., & Li, C. (2013). 3D carbon based nanostructures for advanced supercapacitors. *Energy & Environmental Science*, *6*(1), 41-53.
- [4] Simon, P., & Gogotsi, Y. (2010). Materials for electrochemical capacitors. In *Nanoscience And Technology: A Collection of Reviews from Nature Journals* (pp. 320-329).
- [5] Augustyn, V., Simon, P., & Dunn, B. (2014). Pseudocapacitive oxide materials for high-rate electrochemical energy storage. *Energy & Environmental Science*, *7*(5), 1597-1614.
- [6] Wang, G., Zhang, L., & Zhang, J. (2012). A review of electrode materials for electrochemical supercapacitors. *Chemical Society Reviews*, *41*(2), 797-828.
- [7] Wu, Z., Li, L., Yan, J. M., & Zhang, X. B. (2017). Materials Design and System Construction for Conventional and New-Concept Supercapacitors. *Advanced science*, *4*(6), 1600382.
- [8] Nitta, N., Wu, F., Lee, J. T., & Yushin, G. (2015). Li-ion battery materials: present and future. *Materials today*, *18*(5), 252-264.
- [9] Whittingham, S. M. (1976). *U.S. Patent No. US4009052A*. Washington, DC: U.S. Patent and Trademark Office.

- [10] Rao, B. M. L., Francis, R. W., & Christopher, H. A. (1977). Lithium-aluminum electrode. *Journal of The Electrochemical Society*, 124(10), 1490-1492.
- [11] Yoshino, A., Sanechika, K., & Nakajima, T. (1985). USP4, 668,595, 1985; A. Yoshino, K. Sanechika, T. Nakajima, JP1989293.
- [12] Goodenough, J. B. (2018). How we made the Li-ion rechargeable battery. *Nature Electronics*, 1(3), 204.
- [13] Fuller, T. F., & Harb, J. N. (2018). *Electrochemical engineering*. John Wiley & Sons.
- [14] Wagner, R., Preschitschek, N., Passerini, S., Leker, J., & Winter, M. (2013). Current research trends and prospects among the various materials and designs used in lithium-based batteries. *Journal of Applied Electrochemistry*, 43(5), 481-496.
- [15] Jin, Y., Zhu, B., Lu, Z., Liu, N., & Zhu, J. (2017). Challenges and Recent Progress in the Development of Si Anodes for Lithium-Ion Battery. *Advanced Energy Materials*, 7(23), 1700715.
- [16] Peng, L., Zhu, Y., Chen, D., Ruoff, R. S., & Yu, G. (2016). Two-Dimensional Materials for Beyond-Lithium-Ion Batteries. *Advanced Energy Materials*, 6(11), 1600025.
- [17] Nam, K. T., Kim, D. W., Yoo, P. J., Chiang, C. Y., Meethong, N., Hammond, P. T., ... & Belcher, A. M. (2006). Virus-enabled synthesis and assembly of nanowires for lithium ion battery electrodes. *science*, 312(5775), 885-888.
- [18] Whittingham, M. S. (2004). Lithium batteries and cathode materials. *Chemical reviews*, 104(10), 4271-4302.

- [19] Gurung, A., Chen, K., Khan, R., Abdulkarim, S. S., Varnekar, G., Pathak, R., ... & Qiao, Q. (2017). Highly efficient perovskite solar cell photocharging of lithium ion battery using DC–DC booster. *Advanced Energy Materials*, 7(11), 1602105.
- [20] Wang, H., & Dai, H. (2013). Strongly coupled inorganic–nano-carbon hybrid materials for energy storage. *Chemical Society Reviews*, 42(7), 3088-3113.
- [21] Park, K., Yu, B. C., & Goodenough, J. B. (2016). Li₃N as a Cathode Additive for High-Energy-Density Lithium-Ion Batteries. *Advanced Energy Materials*, 6(10), 1502534.
- [22] Chae, S., Kim, N., Ma, J., Cho, J., & Ko, M. (2017). One-to-One Comparison of Graphite-Blended Negative Electrodes Using Silicon Nanolayer-Embedded Graphite versus Commercial Benchmarking Materials for High-Energy Lithium-Ion Batteries. *Advanced Energy Materials*, 7(15), 1700071.
- [23] Mahmood, N., Tang, T., & Hou, Y. (2016). Nanostructured anode materials for lithium ion batteries: progress, challenge and perspective. *Advanced Energy Materials*, 6(17), 1600374.
- [24] Zhang, X., Tang, Y., Zhang, F., & Lee, C. S. (2016). A Novel Aluminum–Graphite Dual-Ion Battery. *Advanced Energy Materials*, 6(11), 1502588.
- [25] Lochala, J. A., Zhang, H., Wang, Y., Okolo, O., Li, X., & Xiao, J. (2017). Practical Challenges in Employing Graphene for Lithium-Ion Batteries and Beyond. *Small Methods*, 1(6), 1700099.
- [26] Yu, X. Y., Yu, L., & Lou, X. W. (2017). Hollow nanostructures of molybdenum sulfides for electrochemical energy storage and conversion. *Small Methods*, 1(1-2), 1600020.

- [27]Zhao, Y., Li, X., Yan, B., Xiong, D., Li, D., Lawes, S., & Sun, X. (2016). Recent developments and understanding of novel mixed transition-metal oxides as anodes in lithium ion batteries. *Advanced Energy Materials*, 6(8), 1502175.
- [28]Schmuck, R., Wagner, R., Hörpel, G., Placke, T., & Winter, M. (2018). Performance and cost of materials for lithium-based rechargeable automotive batteries. *Nature Energy*, 3(4), 267.
- [29]Placke, T., Heckmann, A., Schmuck, R., Meister, P., Beltrop, K., & Winter, M. (2018). Perspective on performance, cost, and technical challenges for practical dual-ion batteries. *Joule*.
- [30]Rudorff, W., & Hofmann, U. (1938). Über graphitsaltze. *Z. Anorg. Allg. Chem*, 238(1), 1-50.
- [31]McCullough Jr, F. P., & Beale Jr, A. F. (1989). *U.S. Patent No. 4,865,931*. Washington, DC: U.S. Patent and Trademark Office.
- [32]McCullough, F. P., Levine, A., & Snelgrove, R. V. (1989). US Pat., 4830938, 1989;(b) FP McCullough and AF Beale. *US Pat, 4865931*.
- [33]McCullough, F. P. (1996). *U.S. Patent No. 5,518,836*. Washington, DC: U.S. Patent and Trademark Office.
- [34]McCullough, F. P. (1996). *U.S. Patent No. 5,532,083*. Washington, DC: U.S. Patent and Trademark Office.
- [35]Carlin, R. T., Hugh, C., Fuller, J., & Trulove, P. C. (1994). Dual intercalating molten electrolyte batteries. *Journal of the Electrochemical Society*, 141(7), L73-L76.
- [36]Rothermel, S., Meister, P., Schmuelling, G., Fromm, O., Meyer, H. W., Nowak,

- S., ... & Placke, T. (2014). Dual-graphite cells based on the reversible intercalation of bis (trifluoromethanesulfonyl) imide anions from an ionic liquid electrolyte. *Energy & Environmental Science*, 7(10), 3412-3423.
- [37] Santhanam, R., & Noel, M. (1995). Electrochemical intercalation of ionic species of tetrabutylammonium perchlorate on graphite electrodes. A potential dual-intercalation battery system. *Journal of power sources*, 56(1), 101-105.
- [38] Sheng, M., Zhang, F., Ji, B., Tong, X., & Tang, Y. (2017). A novel tin-graphite dual-ion battery based on sodium-ion electrolyte with high energy density. *Advanced Energy Materials*, 7(7), 1601963.
- [39] Lin, M. C., Gong, M., Lu, B., Wu, Y., Wang, D. Y., Guan, M., ... & Dai, H. (2015). An ultrafast rechargeable aluminium-ion battery. *Nature*, 520(7547), 324.
- [40] Wang, S., Jiao, S., Song, W. L., Chen, H. S., Tu, J., Tian, D., ... & Fang, D. N. (2018). A novel dual-graphite aluminum-ion battery. *Energy Storage Materials*, 12, 119-127.
- [41] Seel, J. A., & Dahn, J. R. (2000). Electrochemical intercalation of PF₆ into graphite. *Journal of the Electrochemical Society*, 147(3), 892-898.
- [42] Placke, T., Bieker, P., Lux, S. F., Fromm, O., Meyer, H. W., Passerini, S., & Winter, M. (2012). Dual-ion cells based on anion intercalation into graphite from ionic liquid-based electrolytes. *Zeitschrift für Physikalische Chemie*, 226(5-6), 391-407.
- [43] Read, J. A., Cresce, A. V., Ervin, M. H., & Xu, K. (2014). Dual-graphite chemistry enabled by a high voltage electrolyte. *Energy & Environmental Science*, 7(2), 617-620.
- [44] Ji, B., Zhang, F., Song, X., & Tang, Y. (2017). A Novel Potassium-Ion-Based

- Dual-Ion Battery. *Advanced materials*, 29(19), 1700519.
- [45] Ji, B., Zhang, F., Wu, N., & Tang, Y. (2017). A Dual-Carbon Battery Based on Potassium-Ion Electrolyte. *Advanced Energy Materials*, 7(20), 1700920.
- [46] Meister, P., Siozios, V., Reiter, J., Klamor, S., Rothermel, S., Fromm, O., ... & Placke, T. (2014). Dual-ion cells based on the electrochemical intercalation of asymmetric fluorosulfonyl-(trifluoromethanesulfonyl) imide anions into graphite. *Electrochimica Acta*, 130, 625-633.
- [47] Placke, T., Fromm, O., Rothermel, S., Schmuelling, G., Meister, P., Meyer, H. W., ... & Winter, M. (2013). Electrochemical intercalation of bis (trifluoromethanesulfonyl) imide anion into various graphites for dual-ion cells. *ECS Transactions*, 50(24), 59-68.
- [48] Placke, T., Schmuelling, G., Kloepsch, R., Meister, P., Fromm, O., Hilbig, P., ... & Winter, M. (2014). In situ X-ray Diffraction Studies of Cation and Anion Intercalation into Graphitic Carbons for Electrochemical Energy Storage Applications. *Zeitschrift für anorganische und allgemeine Chemie*, 640(10), 1996-2006.
- [49] Placke, T., Fromm, O., Lux, S. F., Bieker, P., Rothermel, S., Meyer, H. W., ... & Winter, M. (2012). Reversible intercalation of bis (trifluoromethanesulfonyl) imide anions from an ionic liquid electrolyte into graphite for high performance dual-ion cells. *Journal of the Electrochemical Society*, 159(11), A1755-A1765.
- [50] Placke, T., Rothermel, S., Fromm, O., Meister, P., Lux, S. F., Huesker, J., ... & Winter, M. (2013). Influence of graphite characteristics on the electrochemical intercalation of bis (trifluoromethanesulfonyl) imide anions into a graphite-based

- cathode. *Journal of the Electrochemical Society*, 160(11), A1979-A1991.
- [51] Schmuelling, G., Placke, T., Kloepsch, R., Fromm, O., Meyer, H. W., Passerini, S., & Winter, M. (2013). X-ray diffraction studies of the electrochemical intercalation of bis (trifluoromethanesulfonyl) imide anions into graphite for dual-ion cells. *Journal of Power Sources*, 239, 563-571.
- [52] Rothermel, S., Meister, P., Fromm, O., Huesker, J., Meyer, H. W., Winter, M., & Placke, T. (2014). Study of the electrochemical behavior of dual-graphite cells using ionic liquid-based electrolytes. *ECS Transactions*, 58(14), 15-25.
- [53] Aubrey, M. L., & Long, J. R. (2015). A dual-ion battery cathode via oxidative insertion of anions in a metal-organic framework. *Journal of the American Chemical Society*, 137(42), 13594-13602.
- [54] Wang, M., & Tang, Y. (2018). A Review on the Features and Progress of Dual-Ion Batteries. *Advanced Energy Materials*, 8(19), 1703320.
- [55] Neto, A. C., Guinea, F., Peres, N. M., Novoselov, K. S., & Geim, A. K. (2009). The electronic properties of graphene. *Reviews of modern physics*, 81(1), 109.
- [56] Ferrari, A. C. (2007). Raman spectroscopy of graphene and graphite: disorder, electron-phonon coupling, doping and nonadiabatic effects. *Solid state communications*, 143(1-2), 47-57.
- [57] Ishihara, T., Koga, M., Matsumoto, H., & Yoshio, M. (2007). Electrochemical intercalation of hexafluorophosphate anion into various carbons for cathode of dual-carbon rechargeable battery. *Electrochemical and solid-state letters*, 10(3), A74-A76.
- [58] Tarascon, J. M., & Armand, M. (2011). Issues and challenges facing rechargeable

- lithium batteries. In *Materials for Sustainable Energy: A Collection of Peer-Reviewed Research and Review Articles from Nature Publishing Group* (pp. 171-179).
- [59] Poizot, P., & Dolhem, F. (2011). Clean energy new deal for a sustainable world: from non-CO₂ generating energy sources to greener electrochemical storage devices. *Energy & Environmental Science*, 4(6), 2003-2019.
- [60] Armand, M., & Tarascon, J. M. (2008). Building better batteries. *nature*, 451(7179), 652.
- [61] Pérez, I. A. R., Jian, Z., Waldenmaier, P. K., Palmisano, J. W., Chandrabose, R. S., Wang, X., ... & Ji, X. (2017, April). A Hydrocarbon Cathode for Dual-Ion Batteries. In *Meeting Abstracts* (No. 5, pp. 454-454). The Electrochemical Society.
- [62] Dong, X., Yu, H., Ma, Y., Bao, J. L., Truhlar, D. G., Wang, Y., & Xia, Y. (2017). All-Organic Rechargeable Battery with Reversibility Supported by “Water-in-Salt” Electrolyte. *Chemistry—A European Journal*, 23(11), 2560-2565.
- [63] Song, Z., & Zhou, H. (2013). Towards sustainable and versatile energy storage devices: an overview of organic electrode materials. *Energy & Environmental Science*, 6(8), 2280-2301.
- [64] Zhu, L. M., Lei, A. W., Cao, Y. L., Ai, X. P., & Yang, H. X. (2013). An all-organic rechargeable battery using bipolar polyparaphenylene as a redox-active cathode and anode. *Chemical Communications*, 49(6), 567-569.
- [65] Lee, M., Hong, J., Lee, B., Ku, K., Lee, S., Park, C. B., & Kang, K. (2017). Multi-electron redox phenazine for ready-to-charge organic batteries. *Green Chemistry*, 19(13), 2980-2985.

- [66] Schon, T. B., McAllister, B. T., Li, P. F., & Seferos, D. S. (2016). The rise of organic electrode materials for energy storage. *Chemical Society Reviews*, *45*(22), 6345-6404.
- [67] Liang, Y., Tao, Z., & Chen, J. (2012). Organic electrode materials for rechargeable lithium batteries. *Advanced Energy Materials*, *2*(7), 742-769.
- [68] Speer, M. E., Kolek, M., Jassoy, J. J., Heine, J., Winter, M., Bieker, P. M., & Esser, B. (2015). Thianthrene-functionalized polynorbornenes as high-voltage materials for organic cathode-based dual-ion batteries. *Chemical Communications*, *51*(83), 15261-15264.
- [69] Beck, J., Bredow, T., & Tjahjanto, R. T. (2009). Thianthrene Radical Cation Hexafluorophosphate. *Zeitschrift für Naturforschung B*, *64*(2), 145-152.
- [70] Tinker, L. A., & Bard, A. J. (1979). Electrochemistry in liquid sulfur dioxide. 1. Oxidation of thianthrene, phenothiazine, and 9, 10-diphenylanthracene. *Journal of the American Chemical Society*, *101*(9), 2316-2319.
- [71] Hammerich, O., & Parker, V. D. (1973). The reversible oxidation of aromatic cation radicals to dications. Solvents of low nucleophilicity. *Electrochimica Acta*, *18*(8), 537-541.
- [72] Dong, S., Li, Z., Rodríguez-Pérez, I. A., Jiang, H., Lu, J., Zhang, X., & Ji, X. (2017). A novel coronene//Na₂Ti₃O₇ dual-ion battery. *Nano Energy*, *40*, 233-239.
- [73] Poizot, P. L. S. G., Laruelle, S., Grugeon, S., Dupont, L., & Tarascon, J. M. (2000). Nano-sized transition-metal oxides as negative-electrode materials for lithium-ion batteries. *Nature*, *407*(6803), 496.
- [74] Thapa, A. K., Park, G., Nakamura, H., Ishihara, T., Moriyama, N., Kawamura,

- T., ... & Yoshio, M. (2010). Novel graphite/TiO₂ electrochemical cells as a safe electric energy storage system. *Electrochimica Acta*, 55(24), 7305-7309.
- [75] Gunawardhana, N., Park, G. J., Dimov, N., Thapa, A. K., Nakamura, H., Wang, H., ... & Yoshio, M. (2011). Constructing a novel and safer energy storing system using a graphite cathode and a MoO₃ anode. *Journal of Power Sources*, 196(18), 7886-7890.
- [76] Gunawardhana, N., Park, G. J., Thapa, A. K., Dimov, N., Sasidharan, M., Nakamura, H., & Yoshio, M. (2012). Performance of a graphite (KS-6)/MoO₃ energy storing system. *Journal of Power Sources*, 203, 257-261.
- [77] Shi, X., Zhang, W., Wang, J., Zheng, W., Huang, K., Zhang, H., ... & Chen, H. (2016). (EMIm)+(PF₆)- Ionic Liquid Unlocks Optimum Energy/Power Density for Architecture of Nanocarbon-Based Dual-Ion Battery. *Advanced Energy Materials*, 6(24), 1601378.
- [78] Zhang, Z., Hu, L., Wu, H., Weng, W., Koh, M., Redfern, P. C., ... & Amine, K. (2013). Fluorinated electrolytes for 5 V lithium-ion battery chemistry. *Energy & Environmental Science*, 6(6), 1806-1810.
- [79] Hu, L., Zhang, Z., & Amine, K. (2013). Fluorinated electrolytes for Li-ion battery: An FEC-based electrolyte for high voltage LiNi_{0.5}Mn_{1.5}O₄/graphite couple. *Electrochemistry communications*, 35, 76-79.
- [80] Liao, Y., Sun, C., Hu, S., & Li, W. (2013). Anti-thermal shrinkage nanoparticles/polymer and ionic liquid based gel polymer electrolyte for lithium ion battery. *Electrochimica Acta*, 89, 461-468.
- [81] Hayes, R., Warr, G. G., & Atkin, R. (2015). Structure and nanostructure in ionic

- liquids. *Chemical reviews*, 115(13), 6357-6426.
- [82] Xiang, J., Wu, F., Chen, R., Li, L., & Yu, H. (2013). High voltage and safe electrolytes based on ionic liquid and sulfone for lithium-ion batteries. *Journal of Power Sources*, 233, 115-120.
- [83] Liu, J., Pang, W. K., Zhou, T., Chen, L., Wang, Y., Peterson, V. K., ... & Xia, Y. (2017). Li₂TiSiO₅: a low potential and large capacity Ti-based anode material for Li-ion batteries. *Energy & Environmental Science*, 10(6), 1456-1464.
- [84] Zhang, S. S. (2017). Eliminating pre-lithiation step for making high energy density hybrid Li-ion capacitor. *Journal of Power Sources*, 343, 322-328.